Inorganic Chemistry
Article

Inorg. Chem. **2010**, *49*, 1111–1121 **1111**
DOI: 10.1021/ic9020542

Amine− and Dimeric Amino−Borane Complexes of the $\{Rh(P^iPr_3)_2\}^+$ Fragment and Their Relevance to the Transition-Metal-Mediated Dehydrocoupling of Amine−Boranes

Adrian B. Chaplin and Andrew S. Weller*

Department of Inorganic Chemistry, University of Oxford, Oxford, OX1 3QR, United Kingdom

Received October 16, 2009

Complexes formed between $\{Rh(P^iPr_3)_2\}^+$ or $\{Rh(H)_2(P^iPr_3)_2\}^+$ fragments and the amine− and dimeric amino−borane σ ligands $H_3B\cdot NMe_3$ and $[H_2BNMe_2]_2$ have been prepared and their solution and solid-state structures determined: $[Rh(P^iPr_3)_2(\eta^2\text{-}H_3B\cdot NMe_3)][BAr^F{}_4]$ (**1**), $[Rh(P^iPr_3)_2\{\eta^2\text{-}(H_2BNMe_2)_2\}][BAr^F{}_4]$ (**2**), $[Rh(H)_2(P^iPr_3)_2(\eta^2\text{-}H_3B\cdot NMe_3)][BAr^F{}_4]$ (**3**), and $[Rh(H)_2(P^iPr_3)_2\{\eta^2\text{-}(H_2BNMe_2)_2\}][BAr^F{}_4]$ (**4**) [$Ar^F = C_6H_3(CF_3)_2$]. The last compound was only observed in the solid state, as in solution it dissociates to give $[Rh(H)_2(P^iPr_3)_2][BAr^F{}_4]$ and $[H_2BNMe_2]_2$ due to steric pressure between the ligand and the metal fragment. The structures and reactivities of these new complexes are compared with the previously reported tri-isobutyl congeners. On the basis of ^{11}B and ^1H NMR spectroscopy in solution and the Rh···B distances measured in the solid state, the P^iPr_3 complexes show tighter interactions with the σ ligands compared to the P^iBu_3 complexes for the Rh(I) species and a greater stability toward H_2 loss for the Rh(III) salts. For the Rh(I) species (**1** and **2**), this is suggested to be due to electronic factors associated with the bending of the ML_2 fragment. For the Rh(III) complexes (**3** and **4**), the underlying reasons for increased stability toward H_2 loss are not as clear, but steric factors are suggested to influence the relative stability toward a loss of dihydrogen, although other factors, such as supporting agostic interactions, might also play a part. These tighter interactions and a slower H_2 loss are reflected in a catalyst that turns over more slowly in the dehydrocoupling of $H_3B\cdot NHMe_2$ to give the dimeric amino−borane $[H_2BNMe_2]_2$, when compared with the P^iBu_3-ligated catalyst (ToF 4 h^{-1}, c.f., 15 h^{-1}, respectively). The addition of excess MeCN to **1**, **2**, or **3** results in the displacement of the σ-ligand and the formation of the adduct species *trans*-$[Rh(P^iPr_3)_2(NCMe)_2][BAr^F{}_4]$ (with **1** and **2**) and the previously reported $[Rh(H)_2(P^iPr_3)_2(NCMe)_2][BAr^F{}_4]$ (with **3**).

1. Introduction

The transition-metal-mediated dehydrocoupling of phosphine− and amine−boranes is of considerable current interest due to the potential to control (a) the kinetics of hydrogen release and (b) the product distributions for the resulting group 13 and 15 materials (e.g., linear oligomeric, cyclic, or polymeric materials).[1] The high gravimetric hydrogen content of $H_3B\cdot NH_3$ has made it an attractive target as a hydrogen-transport vector for future energy requirements,[2−4] and new developments in the regeneration of spent materials offer encouraging strategies for the reuse of these materials.[5] Catalysts from across the transition series of the periodic table have proved effective for the dehydrocoupling of amine−boranes,[6−20] and impressive rates of hydrogen release[13,17] and control over polymer formation[11] have been achieved.

*To whom correspondence should be addressed. E-mail: andrew.weller@chem.ox.ac.uk.

(1) Clark, T. J.; Lee, K.; Manners, I. *Chem.—Eur. J.* **2006**, *12*, 8634–8648.
(2) Marder, T. B. *Angew. Chem., Int. Ed.* **2007**, *46*, 8116–8118.
(3) Hamilton, C. W.; Baker, R. T.; Staubitz, A.; Manners, I. *Chem. Soc. Rev.* **2009**, *38*, 279–293.
(4) Stephens, F. H.; Pons, V.; Baker, R. T. *Dalton Trans.* **2007**, 2613–2626.
(5) Davis, B. L.; Dixon, D. A.; Garner, E. B.; Gordon, J. C.; Matus, M. H.; Scott, B.; Stephens, F. H. *Angew. Chem., Int. Ed.* **2009**, *48*, 6812–6816.
(6) Zahmakiran, M.; Özkar, S. *Inorg. Chem.* **2009**, *48*, 8955–8964.
(7) Sloan, M. E.; Clark, T. J.; Manners, I. *Inorg. Chem.* **2009**, *48*, 2429–2435.
(8) Rousseau, R.; Schenter, G. K.; Fulton, J. L.; Linehan, J. C.; Engelhard, M. H.; Autrey, T. *J. Am. Chem. Soc.* **2009**, *131*, 10516–10524.
(9) Jiang, Y.; Blacque, O.; Fox, T.; Frech, C. M.; Berke, H. *Organometallics* **2009**, *28*, 5493−5504.
(10) Dallanegra, R.; Chaplin, A. B.; Weller, A. S. *Angew. Chem., Int. Ed.* **2009**, *48*, 6875–6878.
(11) Staubitz, A.; Soto, A. P.; Manners, I. *Angew. Chem., Int. Ed.* **2008**, *47*, 6212–6215.
(12) Douglas, T. M.; Chaplin, A. B.; Weller, A. S. *J. Am. Chem. Soc.* **2008**, *130*, 14432–14433.
(13) Blaquiere, N.; Diallo-Garcia, S.; Gorelsky, S. I.; Black, D. A.; Fagnou, K. *J. Am. Chem. Soc.* **2008**, *130*, 14034–14034.
(14) Pun, D.; Lobkovsky, E.; Chirik, P. J. *Chem. Commun.* **2007**, 3297–3299.
(15) Jiang, Y.; Berke, H. *Chem. Commun.* **2007**, 3571–3573.
(16) Fulton, J. L.; Linehan, J. C.; Autrey, T.; Balasubramanian, M.; Chen, Y.; Szymczak, N. K. *J. Am. Chem. Soc.* **2007**, *129*, 11936–11949.
(17) Denney, M. C.; Pons, V.; Hebden, T. J.; Heinekey, D. M.; Goldberg, K. I. *J. Am. Chem. Soc.* **2006**, *128*, 12048–12049.
(18) Clark, T. J.; Russell, C. A.; Manners, I. *J. Am. Chem. Soc.* **2006**, *128*, 9582–9583.
(19) Kawano, Y.; Uruichi, M.; Shimoi, M.; Taki, S.; Kawaguchi, T.; Kakizawa, T.; Ogino, H. *J. Am. Chem. Soc.* **2009**, *131*, 14946−14957.
(20) Keaton, R. J.; Blacquiere, J. M.; Baker, R. T. *J. Am. Chem. Soc.* **2007**, *129*, 1844–1845.

Published on Web 01/06/2010

Chart 1.[a]

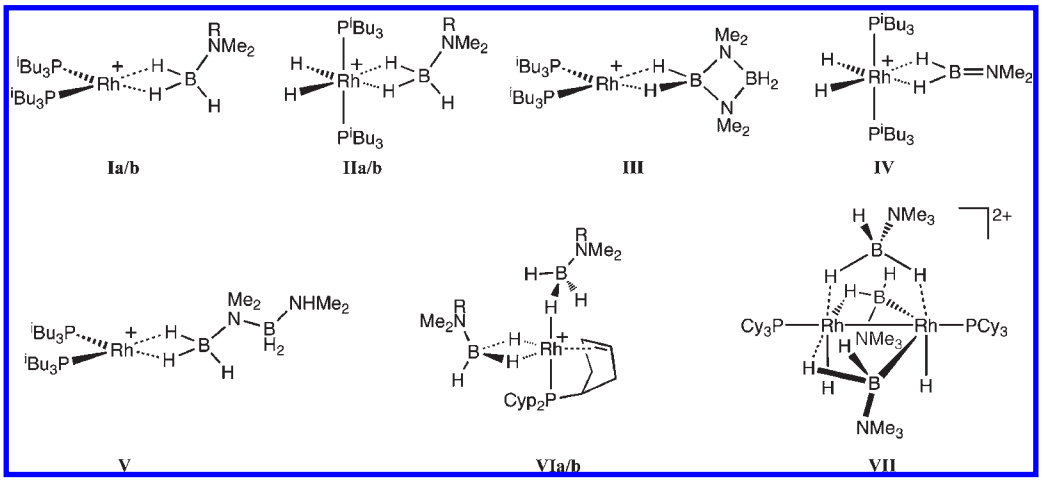

[a] R = H (a), Me (b). $[BAr^F{}_4]^-$ anions are not shown.

Mechanistic investigations using computational[19,21−26] and empirical studies[27−29] indicate a complex process that first involves dehydrogenation of $H_3B\cdot NR_2H$ at a metal center to form an amino−borane $H_2B{=}NR_2$. This process may be inner-sphere (i.e., involving BH/NH transfer pathways at the metal), that is, single-site, colloidal,[27,30,31] or small cluster mediated.[8,16] It can also be outer-sphere, which is related to alcohol oxidation, in which a ligand is also involved in hydrogen transfer.[13,19,32] Subsequent oligomerization, polymerization, or dimerization of $H_2B{=}NMe_2$ can then occur, either on or off the metal (all with the possible further involvement of $H_3B\cdot NR_2H$). Although the details of this and further steps toward the formation of oligomeric and polymeric materials are considerably less-well resolved for metal-based processes,[24,27−29,33,34] off-metal dehydrocoupling has received more attention with regard to the overall mechansim.[22,23,35,36] Hydrolytic processes catalyzed by transition metal complexes have also been reported.[37−40]

Scheme 1. Dehydrocoupling of Amine−Boranes $H_3B\cdot NMeRH$

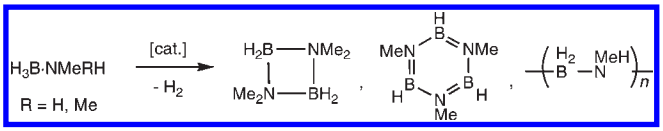

In an effort to understand the mechanistic scenario for amine−borane dehydrogenation in more detail, we have recently reported intermediate and model species that result from cationic $\{Rh(P^iBu_3)_2\}^+$ fragments partnered with $H_3B\cdot NRMe_2$ (R = H, Me), $H_2B{=}NMe_2$, $H_3B\cdot NMe_2BH_2\cdot NHMe_2$, and $[H_2BNMe_2]_2$ ligands.[12,24] Examples of these "unstretched" σ complexes[41] of Rh(I) and Rh(III) are shown in Chart 1 (**I**−**V**). Bis-amine−borane motifs (**VI**)[10] and products of B−H activation (**VII**)[42] have also recently been described by us. These complexes build upon the pioneering work by Shimoi and co-workers on the synthesis of amine−borane and phosphine−borane σ complexes with a variety of transition metal fragments.[43−46] With regard to the dehydrocoupling of $H_3B\cdot NHMe_2$ to cyclic $[H_2BNMe_2]_2$ (Scheme 1) catalyzed by $[Rh(P^iBu_3)_2][BAr^F{}_4]$ [$Ar^F = C_6H_3(CF_3)_2$], complexes **Ia**, **IIa**, **IV,** and **V** all potentially sit on the catalytic cycle. Calculations[24] indicate a complex multipathway process in which the likely first steps are sequential BH/NH or NH/BH activation at the Rh(I) center, following initial formation of a simple amine−borane σ complex

(21) Yang, X.; Hall, M. B. *J. Organomet. Chem.* **2009**, *694*, 2831–2838.
(22) Zimmerman, P. M.; Paul, A.; Zhang, Z. Y.; Musgrave, C. B. *Angew. Chem., Int. Ed.* **2009**, *48*, 2201–2205.
(23) Zimmerman, P. M.; Paul, A.; Zhang, Z. Y.; Musgrave, C. B. *Inorg. Chem.* **2009**, *48*, 1069–1081.
(24) Douglas, T. M.; Chaplin, A. B.; Weller, A. S.; Yang, X. Z.; Hall, M. B. *J. Am. Chem. Soc.* **2009**, *131*, 15440–15456.
(25) Paul, A.; Musgrave, C. B. *Angew. Chem., Int. Ed.* **2007**, *46*, 8153–8156.
(26) Luo, Y.; Ohno, K. *Organometallics* **2007**, *26*, 3597–3600.
(27) Jaska, C. A.; Temple, K.; Lough, A. J.; Manners, I. *J. Am. Chem. Soc.* **2003**, *125*, 9424–9434.
(28) Pons, V.; Baker, R. T.; Szymczak, N. K.; Heldebrant, D. J.; Linehan, J. C.; Matus, M. H.; Grant, D. J.; Dixon, D. A. *Chem. Commun.* **2008**, 6597–6599.
(29) Friedrich, A.; Drees, M.; Schneider, S. *Chem.—Eur. J.* **2009**, *15*, 10339–10342.
(30) Jaska, C. A.; Clark, T. J.; Clendenning, S. B.; Grozea, D.; Turak, A.; Lu, Z.-H.; Manners, I. *J. Am. Chem. Soc.* **2005**, *127*, 5116–5124.
(31) Jaska, C. A.; Manners, I. *J. Am. Chem. Soc.* **2004**, *126*, 9776–9785.
(32) Kass, M.; Friedrich, A.; Drees, M.; Schneider, S. *Angew. Chem., Int. Ed.* **2009**, *48*, 905–907.
(33) Dietrich, B. L.; Goldberg, K. I.; Heinekey, D. M.; Autrey, T.; Linehan, J. C. *Inorg. Chem.* **2008**, *47*, 8583–8585.
(34) Hebden, T. J.; Denney, M. C.; Pons, V.; Piccoli, P. M. B.; Koetzle, T. F.; Schultz, A. J.; Kaminsky, W.; Goldberg, K. I.; Heinekey, D. M. *J. Am. Chem. Soc.* **2008**, *130*, 10812–10820.
(35) Shaw, W. J.; Linehan, J. C.; Szymczak, N. K.; Heldebrant, D. J.; Yonker, C.; Camaioni, D. M.; Baker, R. T.; Autrey, T. *Angew. Chem., Int. Ed.* **2008**, *47*, 7493–7496.
(36) Staubitz, A.; Besora, M.; Harvey, J. N.; Manners, I. *Inorg. Chem.* **2008**, *47*, 5910–5918.
(37) Yan, J. M.; Zhang, X. B.; Han, S.; Shioyama, H.; Xu, Q. *Angew. Chem., Int. Ed.* **2008**, *47*, 2287–2289.
(38) Yoon, C. W.; Sneddon, L. G. *J. Am. Chem. Soc.* **2006**, *128*, 13992–13993.
(39) Clark, T. J.; Whittell, G. R.; Manners, I. *Inorg. Chem.* **2007**, *46*, 7522–7527.
(40) Li, Y.; Xie, L.; Li, Y.; Zheng, J.; Li, X. *Chem.—Eur. J.* **2010**, *15*, 8951–8954.
(41) Kubas, G. J. *Metal Dihydrogen and σ-Bond Complexes*; Kluwer Academic/Plenum Publishers: New York, 2001.
(42) Chaplin, A. B.; Weller, A. S. *Angew. Chem., Int. Ed.* **2009**, DOI: 10.1002/anie.200905185.
(43) Kawano, Y.; Yamaguchi, K.; Miyake, S. Y.; Kakizawa, T.; Shimoi, M. *Chem.—Eur. J.* **2007**, *13*, 6920–6931.
(44) Kawano, Y.; Hashiva, M.; Shimoi, M. *Organometallics* **2006**, *25*, 4420–4426.
(45) Kakizawa, T.; Kawano, Y.; Shimoi, M. *Organometallics* **2001**, *20*, 3211–3213.
(46) Shimoi, M.; Nagai, S.; Ichikawa, M.; Kawano, Y.; Katoh, K.; Uruichi, M.; Ogino, H. *J. Am. Chem. Soc.* **1999**, *121*, 11704–11712.

Scheme 2. Synthesis of **1** and **2**[a]

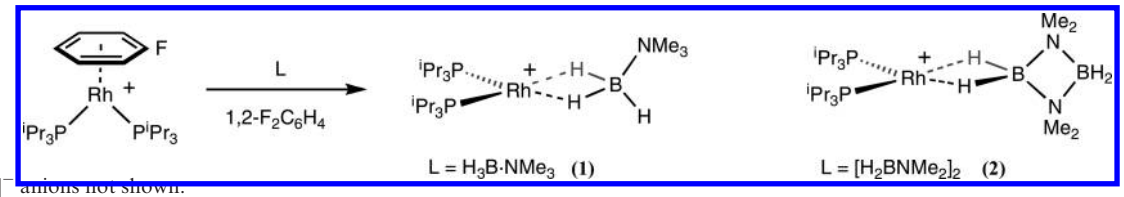

[a] $[BAr^F_4]^-$ anions not shown.

(e.g., **Ia**). Consistent with their observation during and at the end of catalysis, calculations indicate that **IIa** and **IV** sit in relatively deep energy wells.

Given that these well-defined complexes of amine−boranes could be prepared using the $\{Rh(P^iBu_3)_2\}^+$ fragment, we were interested in varying the steric and electronic profile of the phosphine to probe the consequences (if any) on observed ground state structures and the rate of catalysis for the dehydrocoupling of $H_3B\cdot NHMe_2$. For our first attempt at this, we turned to model complexes based upon the $\{Rh(P^iPr_3)_2\}^+$ and $\{Rh(H)_2(P^iPr_3)_2\}^+$ fragments partnered with the amine−borane $H_3B\cdot NMe_3$ or, the ultimate product of $H_3B\cdot NMe_2H$ dehydrogenation, the cyclic amino−borane $[H_2BNMe_2]_2$. Solid-state and solution studies allow a comparison between these complexes and those of P^iBu_3. Despite the steric and electronic similarity between P^iBu_3 and P^iPr_3,[47] there is a subtle, but distinct, change in the strength of interaction between these ligands and the metal centers in the Rh(I) complexes, as measured by NMR spectroscopy and X-ray crystallography, as well as the ease of reductive elimination of H_2 from the Rh(III) dihydride complexes. We also demonstrate an attenuation in the rate of dehydrocoupling of $H_3B\cdot NHMe_2$ to form cyclic $[H_2BNMe_2]_2$ when using the ^{t}Pr-substituted catalyst.

Studies of single-site transition-metal catalyzed-amine−borane dehydrogenation where the ligand set or metal has been varied have been reported previously; these have generally focused upon the relative rates of catalysis rather than the isolation, per se, of likely intermediates or models thereof.[7,9,15,19,20] Systematic studies on the coordination properties of $H_2RB\cdot L$ (R = Cl, H, Me, Ph; L = PMe_3, NMe_3, PPh_3, for example) have also been reported.[43]

Some of these complexes have been briefly described in a recent communication.[42]

2. Results

2.1. Synthesis of Rh(I) Complexes of $H_3B\cdot NMe_3$ and $[H_2BNMe_2]_2$. The substrate $H_3B\cdot NMe_3$ does not contain a NH group, and thus dehydrocoupling at a transition metal center cannot proceed. This enables the isolation of relatively stable and long-lived complexes. Reaction of $H_3B\cdot NMe_3$ with $[Rh(P^iPr_3)_2(\eta^6\text{-}C_6H_5F)][BAr^F_4]$[48] in 1,2-$F_2C_6H_4$ solution led to the immediate formation of the new complex $[Rh(P^iPr_3)_2(\eta^2\text{-}H_3B\cdot NMe_3)][BAr^F_4]$ (**1**) and elimination of C_6H_5F. Similarly, reaction of the cyclic dimer $[H_2BNMe_2]_2$[27] with $[Rh(P^iPr_3)_2(\eta^6\text{-}C_6H_5F)][BAr^F_4]$ afforded $[Rh(P^iPr_3)_2\{\eta^2\text{-}(H_2BNMe_2)_2\}][BAr^F_4]$ (**2**; Scheme 2). Both **1** and **2** are isolated as purple, air-sensitive, crystalline solids in good yields. They are direct analogs of the P^iBu_3 ligated complexes **Ib** and **III** (Chart 1). Their solid-state structures are shown in Figures 1 and 2, respectively. For **2**, there are two independent ion pairs in the unit cell,

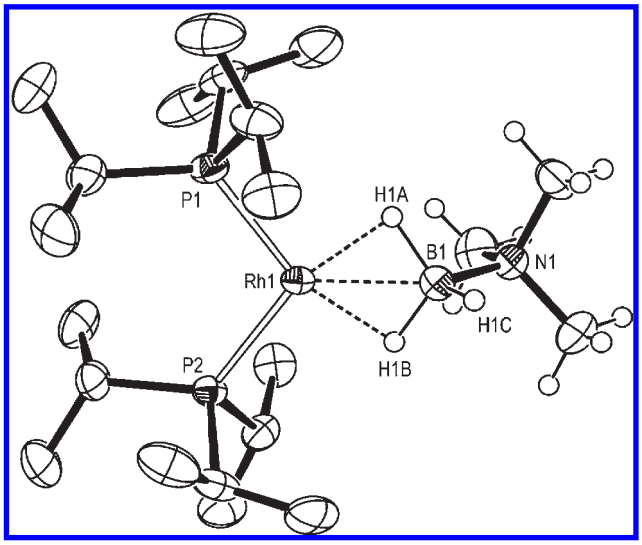

Figure 1. Cationic portion of **1**. Thermal ellipsoids shown at the 50% probability level. Phosphine H atoms omitted for clarity. Selected bond lengths (Å) and angles (deg): Rh1−B1, 2.1376(3); B1−H1A, 1.22(4); B1−H1B, 1.22(4); B1−H1C, 1.13(6); B1−N1, 1.594(7); Rh1−P1, 2.2478(12); Rh1−P2, 2.2679(12); P1−Rh1−P2, 106.08(5); Rh1−B1−N1, 131.5(4); H1A−Rh1−H1B, 68(3).

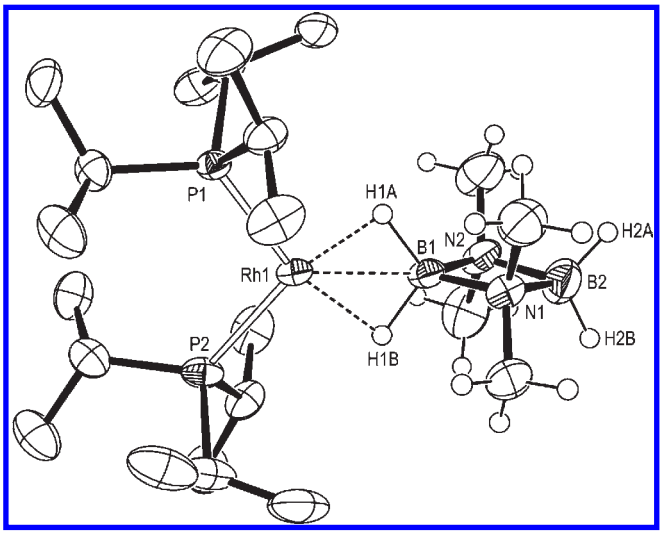

Figure 2. Cationic portion of one of the crystallographically independent cations in the unit cell for **2**. Thermal ellipsoids shown at the 50% probability level. Phosphine H atoms omitted for clarity. Selected bond lengths (Å) and angles (deg): Rh1−B1, 2.124(4); B1−H1A, 1.23(2); B1−H1B, 1.24(2); Rh1−P1, 2.2681(8); Rh1−P2, 2.2883(9); P1−Rh1−P2, 105.61(3). Second independent molecule: Rh2−B11, 2.118(4); P3−Rh2−P4, 107.14(3).

(47) Tolman, C. A. *Chem. Rev.* **1977**, *77*, 313–348.
(48) Chaplin, A. B.; Poblador-Bahamonde, A. I.; Sparkes, H. A.; Howard, J. A. K.; Macgregor, S. A.; Weller, A. S. *Chem. Commun.* **2009**, 244–246.

Table 1. Comparison of Selected Structural and Spectroscopic Data[a] for the P^iPr_3 (**1**–**5**) and P^iBu_3 Complexes (**Ia**, **IIa/b**, **III**)[24]

	d(Rh−B)/Å	P−Rh−P/deg	$\delta(^{11}B)$	$\Delta\delta(^{11}B)^b$	*J*(HB)/Hz[c]	$\delta(^1H)$ Rh−*H*−B, Rh−*H*[d]
1	2.137(6)	106.08(5)	28.8	+36.1	80	−3.09, n/a (−6.91)
Ib	2.180(4)	97.35(4)	23.1	+30.4	*d*	−2.12, n/a (−5.55)
2	2.124(4)	105.61(3)	35.3	+29.8	89	−6.50, n/a
	2.118(4)	107.14(3)[e]				
III	2.161(6)	98.31(6)	31.1	+25.6	89	−5.07, n/a
	2.140(7)[e]	94.42(5)[e]				
3	2.325(4)	157.05(3)	5.0	+12.3	80	−0.57, −19.75
IIb	*f*	*f*	5.1	+12.4	*g*	−0.47, −18.81
4	2.386(15)	151.11(15)	*h*	*h*	*h*	*h*
5	*f*	*f*	3.2	+16.0	*g*	−1.0, −18.15 (−3.56)
IIa	2.318(8)	163.65(7)	2.2	+15.0	*g*	−0.77, −17.42 (−3.15)

[a] Data for **1**−**5** were collected in a CD_2Cl_2 solution, and for **I**−**III** in 1,2-$F_2C_6H_4$, except for low-temperature data (CD_2Cl_2). Comparison of ^{11}B and ^1H chemical shifts for the new complexes in both solvents show only small chemical shift differences (∼0.4 ppm, ^{11}B; ∼0.1 ppm, ^1H). [b] Difference in chemical shift from free ligand: $\delta(^{11}B)$ $H_3B{\cdot}NMe_3$, −7.3 [*J*(HB) 98 Hz]; $H_3B{\cdot}NHMe_2$, −12.8 [*J*(HB) 96 Hz]; $[H_2BNMe_2]_2$, 5.5 [*J*(HB) 112 Hz], as measured in 1,2-$C_6H_4F_2$.[24] [c] Measured from the ^{11}B NMR spectrum at 298 K. [d] 298 K, Rh−*H*−B in parentheses if low-temperature limit reached, see text. [e] Data for second crystallographically independent molecule in the unit cell. [f] Structural data not available. [g] ^{11}B coupling not resolved—broad peaks. [h] Data not available, complex dissociates in solution, see text.

although the structural metrics are not grossly different between the two.

Both the cations in salts **1** and **2** have pseudo-square-planar Rh(I) centers with cis-phosphines and an η^2-cordinated amine−borane or dimeric amino−borane, each bonding through two three-center, two-electron bonds. The Rh···B distances [2.137(6) and 2.124(4)/2.118(4) Å, respectively] are similar to, but shorter than, those reported for the P^iBu_3 analogs [2.180(4) and 2.161(6)/2.140(7) Å for **Ib** and **III**, respectively]. The P1−Rh1−P2 angle is similar for **1** and **2** [106.08(5)° and 105.61(3)/107.14(3)°, respectively], and both are larger than found for **Ib** [97.35(4)°] and **III** [98.31(6)/94.42(5)°]. The hydrogen atoms associated with the borane/metal were located in all cases, and although within error there is no lengthening of the B−H bonds on coordination, absolute values show a trend for a longer B−H bond on interaction with the metal—as expected.[41] The shorter Rh···B distances suggest a tighter interaction for **1** and **2** compared with that for **Ib** and **III**. Table 1 summarizes these structural metrics. Interestingly, a short Rh···B distance is accompanied by a wider P−Rh−P bond angle.

In solution, **1** and **2** retain the Rh−H−B interactions. The ^1H NMR spectrum for **1** shows, in addition to the expected signals due to anion and ^{i}Pr groups, a broad signal at δ −3.09 (relative integral 3-H) that shows coupling to ^{11}B [*J*(BH) 80 Hz], which collapses into a sharper signal in the $^1H\{^{11}B\}$ NMR spectrum. The observation of a 3-H relative integral signal indicates rapid site exchange between bound and terminal B−H, resulting in a frequency-averaged chemical shift.[46] This is frozen out at 190 K, so that an integral 2-H signal is observed at δ −6.91 for the Rh−*H*−B hydrogens at this temperature. The terminal BH group is observed as a broad, integral 1-H signal at δ 4.43. For **2**, site exchange does not occur at room temperature, and a 2-H relative integral resonance is observed at δ −6.50 that is assigned to the Rh−*H*−B hydrogens, while those due to uncoordinated BH_2 are observed at δ 2.70. The high-field hydride signal in **2** is beautifully resolved in the ^1H NMR spectrum into a multiplet that shows coupling to ^{11}B, ^{31}P, and ^{103}Rh (Figure 3)—which can be simulated[49] as an AA′MNXX′ system: *J*(BH), 89; *J*(RhH), 31; *J*(PH), 30 Hz. Experimentally, decoupling ^{31}P resolves this multiplet into a quartet of doublets (^{11}B and ^{103}Rh coupling), while decoupling ^{11}B resolves it into an apparent 1:2:1 triplet (coupling to 1 × ^{31}P and ^{103}Rh). Presumably, it is the trans $^1H-^{31}P$ coupling that is observed, with the cis coupling small and unresolved. The ^{11}B NMR spectrum of **1** shows a signal at δ 28.8 [*J*(BH) 80 Hz] shifted 36.1 ppm downfield from the free ligand (Table 1) and also shows a reduced coupling constant compared to the free ligand [98 Hz]. That of **2** shows two signals, δ 35.3 [t, *J*(BH) 89 Hz] and 5.3 [t, *J*(BH) 112 Hz], the former also showing a reduced coupling constant, allowing it to be assigned to the boron atom involved in the three-center, two-electron bond with the metal. This signal at δ 35.3 is also shifted 29.8 ppm downfield compared to $[H_2BNMe_2]_2$, while that at δ 5.3 is essentially unshifted. These chemical shifts and the reduction in coupling coupling constant are as expected on coordination of the amine−borane to the metal center.[19,41,46,50,51] In comparison with **Ib** and **III**, **1** and **2** show larger upfield shifts

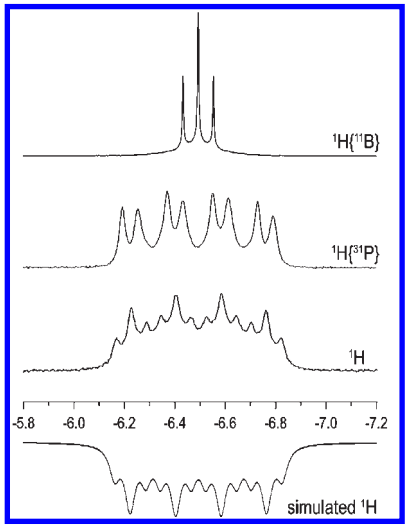

Figure 3. Selected ^1H NMR data for **2** for the Rh−*H*−B resonance centered at δ −6.50 and a simulated (gNMR)[49] spectrum at the bottom.

(49) Budzelaar, P. *gNMR*, 4.0; Cherwell Scientific Publishing, Oxford, 1997.

(50) Alcaraz, G.; Sabo-Etienne, S. *Coord. Chem. Rev.* **2008**, *252*, 2395–2409.

(51) Merle, N.; Koicok-Kohn, G.; Mahon, M. F.; Frost, C. G.; Ruggerio, G. D.; Weller, A. S.; Willis, M. C. *Dalton Trans.* **2004**, 3883–3892.

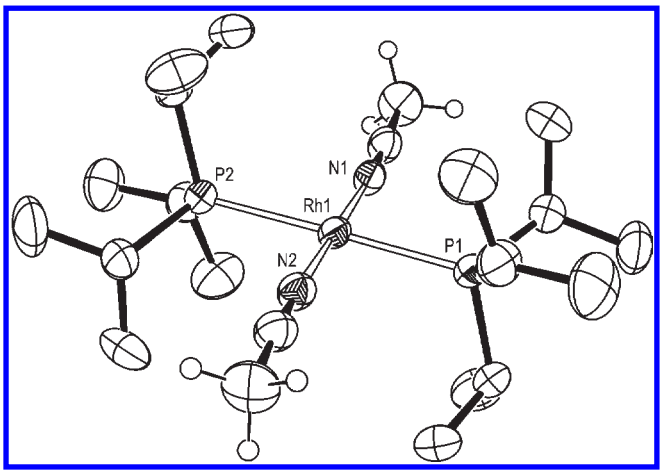

Figure 4. Cationic portion of one of the crystallographically independent cations in the unit cell for *trans*-[Rh(P^iPr_3)$_2$(NCMe)$_2$][BAr^F_4]. Thermal ellipsoids shown at the 50% probability level. Phosphine H atoms omitted for clarity. Selected bond lengths (Å) and angles (deg): Rh1−N1, 1.966(3); Rh1−N2, 1.964(4); Rh1−P1, 2.3353(11); Rh1−P2, 2.3347(10); P1−Rh1−P2, 179.18(4); N1−Rh1−N2, 179.74(14).

for the Rh−*H*−B hydrogens and greater downfield shifts in the ^{11}B NMR spectrum on coordination to the metal fragment. Both are indicative of a stronger interaction in the P^iPr_3 Rh(I) complexes compared to the P^iBu_3 analogs and also correspond with shorter Rh···B distances in the solid state.

The addition of MeCN to a CD_2Cl_2 solution of **1** or **2** results in the displacement of the amine−borane/dimeric amino−borane ligand and the formation of the bis-MeCN adduct [Rh(P^iPr_3)$_2$(NCMe)$_2$][BAr^F_4] as the cis isomer, which converts to the trans over 30 min. The observation of CH*Me*$_2$ protons in the ^{1}H NMR spectrum as an apparent quartet, that collapses to a doublet in the ^{1}H{^{31}P} spectrum, is consistent with this assignment. The solid-state structure is given in Figure 4 and is similar to that reported for *trans*-[Rh(PCy$_3$)$_2$(NCMe)$_2$][BF_4].[52] The Ir analog has also been reported (as the [PF_6]$^-$ salt).[53]

2.2. Synthesis of Rh(III)−Dihydride Complexes of $H_3B\cdot NMe_3$ and [H_2BNMe_2]$_2$. We have previously reported[24] that the addition of H_2 to **Ib** results in the formation of [Rh(H)$_2$(P^iBu_3)$_2$(η^2-$H_3B\cdot NMe_3$)][BAr^F_4] (**IIb**). This complex could not be isolated, as it readily lost H_2 to reform **Ib**, even by simply placing it under an Ar atmosphere. The addition of $H_3B\cdot NMe_3$ to [Rh(H)$_2$(P^iBu_3)$_2$][BAr^F_4], **VIII**, under a H_2 atmosphere also afforded **IIb**. In a similar manner, the addition of H_2 to purple **1** resulted in the immediate formation of a colorless material that was initially characterized spectroscopically as [Rh(H)$_2$(P^iPr_3)$_2$(η^2-$H_3B\cdot NMe_3$)][BAr^F_4] (**3**), by comparison with **IIb**, while combining [Rh(H)$_2$(P^iPr_3)$_2$-(L)$_2$][BAr^F_4] (**IX**, L = agostic interaction or solvent)[54] also afforded **3** (Scheme 3). Interestingly, even though **3** has the bulkier P^iPr_3 phosphine, it does not lose H_2, even when placed under a vacuum for an extended period of time (72 h, 5×10^{-3} Torr), instead requiring a hydrogen acceptor, *tert*-butylethene, to regenerate **1**. This lack of H_2 lability allowed it to be isolated and the solid-state structure to be determined.

The solid-state structure of **3** is shown in Figure 5 and reveals a pseudo-octahedral Rh(III) center, coordinated with trans-phosphines, cis-hydrides, and a σ-$H_3B\cdot NMe_3$ ligand. All hydrogen atoms associated with the metal center were located. The structure is very similar to that reported for [Rh(H)$_2$(P^iBu_3)$_2$(η^2-$H_3B\cdot NHMe_2$)][BAr^F_4] (**IIa**). Although the difference in the amine−borane ligand discourages detailed structural comparisons, the Rh···B distance is the same within error between the two [2.325(4) versus 2.318(8) Å], while the P−Rh−P angle is slightly more acute in **3** [157.05(3) versus 163.65(7)°]. These markers suggest a similar strength of the Rh···B interaction. The solution NMR data for **3** are virtually identical to those of **IIb** (Table 1), showing an upfield-shifted resonance in the ^{11}B NMR spectrum [δ 5.0, shifted 12.3 ppm from the free ligand] on coordination of the borane and a relative integral 3-H signal in the ^{1}H NMR spectrum at δ −0.57, demonstrating site exchange for the H_3B hydrogen atoms. This site exchange cannot be frozen out at 190 K, similar to **IIb**. The hydrides are observed as a sharp relative integral 2-H doublet of triplets at δ −19.75, showing coupling to ^{103}Rh and ^{31}P, which collapse to a doublet in the ^{1}H{^{31}P} NMR spectrum. The observation of only one ^{31}P environment in the ^{31}P{^{1}H} NMR spectrum [δ 64.5; J(RhP), 111 Hz] indicates that the BH site exchange is accompanied by a spin of the amine−borane around the Rh−B vector. These NMR and structural data all point to a weaker Rh−H−B interaction in **3** when compared with the Rh(I) complexes **1** and **2**. This is no doubt due to the increased steric pressure between the borane and the trans phosphine ligands as well as the high-trans-influence hydride ligands. We have noted this previously in complexes **I** and **II**.[24] The addition of MeCN (excess) to **3** results in the immediate formation of the previously reported adduct species [Rh(H)$_2$(P^iPr_3)$_2$(NCMe)$_2$][BAr^F_4][54] via displacement of $H_3B\cdot NMe_3$ (observed).

We have previously reported[24] that complexes of [H_2B-NMe_2]$_2$ could not be observed for the P^iBu_3-ligated complexes of Rh(III)—presumably due to steric pressure between the bulky trans-orientated phosphines and this dimeric amino−borane. Thus, the addition of H_2 to **III** resulted in the formation of **VIII** alongside free [H_2B-NMe_2]$_2$, while in the absence of H_2, the addition of [H_2BNMe_2]$_2$ to **VIII** resulted in the reductive-elimination of H_2 and the isolation of **III**. Similar reactivity is observed for the P^iPr_3 complexes reported here, Scheme 4: the addition of H_2 (1 atm) to **2** results in the formation of **IX** alongside free [H_2BNMe_2]$_2$, and the reaction of [H_2BNMe_2]$_2$ with **IX** resulted in the rapid reductive elimination of H_2 and the formation of **2**. The presence of liberated H_2 from the latter reaction, observed by ^{1}H NMR spectroscopy, results in equilibrium between **IX** and **2** being established—the yield of **2** increasing with added [H_2BNMe_2]$_2$. For example, the reaction of **IX** with 2 equiv of [H_2BNMe_2]$_2$ affords **2** in 80% yield, while with 50 equiv the yield is essentially quantitative. Although this means that the Rh(III)−dihydride complex ligated with [H_2BNMe_2]$_2$, [Rh(H)$_2$(P^iPr_3)$_2${η^2-(H_2BNMe_2)$_2$}][BAr^F_4] (**4**), could not be observed in solution, slow crystallization under a H_2 atmosphere of a mixture of **IX** and [H_2BNMe_2]$_2$

(52) Chisholm, M. H.; Huffman, J. C.; Iyer, S. S. *J. Chem. Soc., Dalton Trans.* **2000**, *9*, 1483–1489.
(53) Dorta, R.; Goikhman, R.; Milstein, D. *Organometallics* **2003**, *22*, 2806–2809.
(54) Ingleson, M. J.; Brayshaw, S. K.; Mahon, M. F.; Ruggiero, G. D.; Weller, A. S. *Inorg. Chem.* **2005**, *44*, 3162–3171.

Scheme 3. Synthesis of **3**[a]

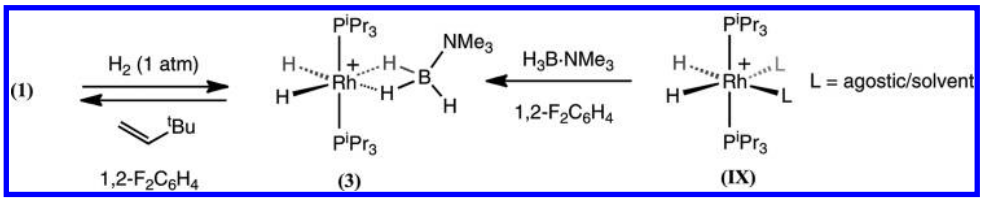

[a] $[BAr^F_4]^-$ anions are not shown.

Scheme 4. Reactivity of **2** and **IX** with $H_2/[H_2BNMe_2]_2$[a]

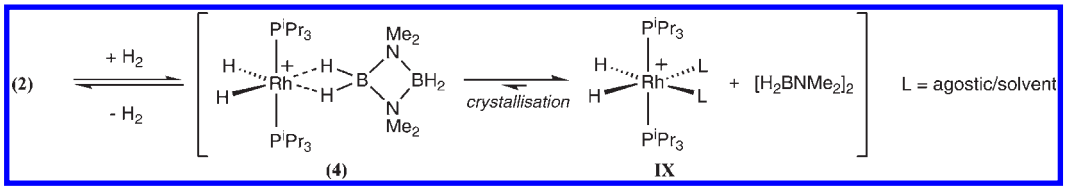

[a] $[BAr^F_4]^-$ anions not shown.

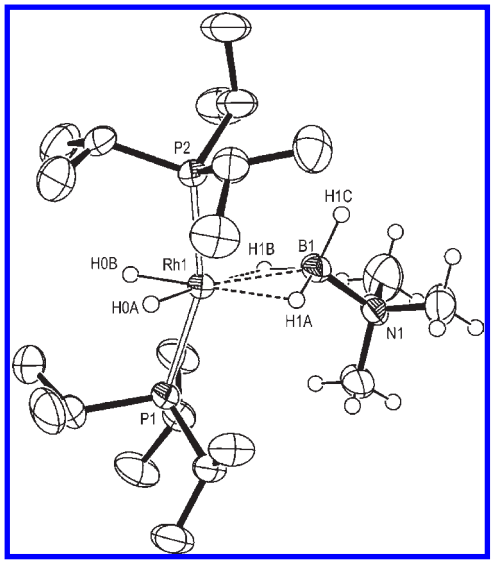

Figure 5. Cationic portion of **3**. Thermal ellipsoids shown at the 50% probability level. Phosphine H atoms and minor disordered component omitted for clarity. Selected bond lengths (Å) and angles (deg): Rh1−B1, 2.325(4); Rh1−H0A, 1.50(3); Rh1−H0B, 1.50(3); B1−H1A, 1.25(3); B1−H1B, 1.25(3); B1−H1C, 1.16(4); Rh1−P1, 2.3259(9); Rh1−P2, 2.3194(9); B1−N1, 1.604(5); P1−Rh1−P2, 157.05(3); Rh1−B1−N1, 137.2(2); H1A−Rh1−H1B, 63(2).

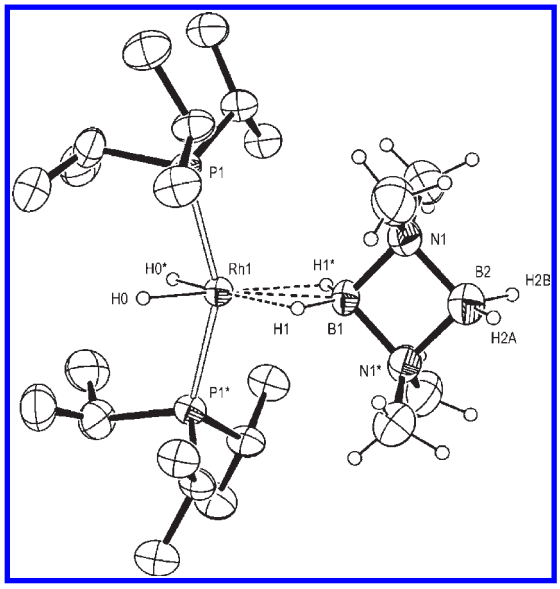

Figure 6. Cationic portion of **4**. Thermal ellipsoids at the 30% probability level. Phosphine H atoms omitted for clarity. Symmetry equivalent atoms (∗) generated by the operation: $y + 1$, $x - 1$, $-z$. Selected bond lengths (Å) and angles (deg): Rh1−B1, 2.386(15); Rh1−P1, 2.343(2); Rh1−H0, 1.44(6); B1−H1, 1.18(8); P1−Rh1−P1, 151.10(14); H1*−Rh1−H1, 59(5).

gave colorless crystals of **4**.[55] This suggests under a H_2 atmosphere an equilibrium exists between **4** and **IX**/$[H_2BNMe_2]_2$, albeit rather one-sided; presumably a lower relative solubility of **4** helps drive the equilibrium to give crystalline material. Redissolving crystalline **4** in CD_2Cl_2 at a low temperature (225 K) afforded a 1:1 mixture of **IX** and $[H_2BNMe_2]_2$ (by NMR spectroscopy). The solid-state structure of **4** is shown in Figure 6 and displays an overall motif similar to that observed for **3**—with trans-phosphine ligands and cis-hydrides. The Rh···B distance, 2.386(15) Å, is the longest of all the complexes discussed here, while the P−Rh−P angle, 151.10(14)°, is the smallest for the Rh(III) complexes. These metrics point to a relatively crowded molecule—consistent with the fact that it can only be observed in the solid state. The observation that H_2 reductive elimination only occurs rapidly when $[H_2BNMe_2]_2$ is added to the Rh(III)−dihydrides **VIII** or **IX** indicates that this occurs from a σ-borane complex, i.e., **4**.

2.3. Catalysis: Dehydrocoupling of $H_3B\cdot NHMe_2$ to $[H_2BNMe_2]_2$. $[Rh(P^iPr_3)_2(\eta^6\text{-}C_6H_5F)][BAr^F_4]$ is a competent precatalyst for the dehydrocoupling of $H_3B\cdot NHMe_2$ [0.072 M initial concentration], to ultimately give $[H_2BNMe_2]_2$. Monitoring this reaction in an open system under

(55) Complex **4** is unstable in the solid state, slowly losing H_2 to form purple **2**. Similarly, the addition of H_2 to **2** in the solid state results in the formation of **4** by a gas/solid reaction (Figure S-1 in the Supporting Information). The addition of H_2 to metal complexes in the solid state has been reported previously: (a) Olivan, M.; Marchenko, A. V.; Coalter, J. N.; Caulton, K. G. *J. Am. Chem. Soc.* **1997**, *119*, 8389–8390. (b) Kubas, G. J.; Unkefer, C. J.; Swanson, B. I.; Fukushima, E. *J. Am. Chem. Soc.* **1986**, *108*, 7000–7009. (c) Matthes, J.; Pery, T.; Grundemann, S.; Buntkowsky, G.; Sabo-Etienne, S.; Chaudret, B.; Limbach, H. H. *J. Am. Chem. Soc.* **2004**, *126*, 8366–8367. (d) Douglas, T. M.; Weller, A. S. *N. J. Chem.* **2008**, *32*, 966–969.

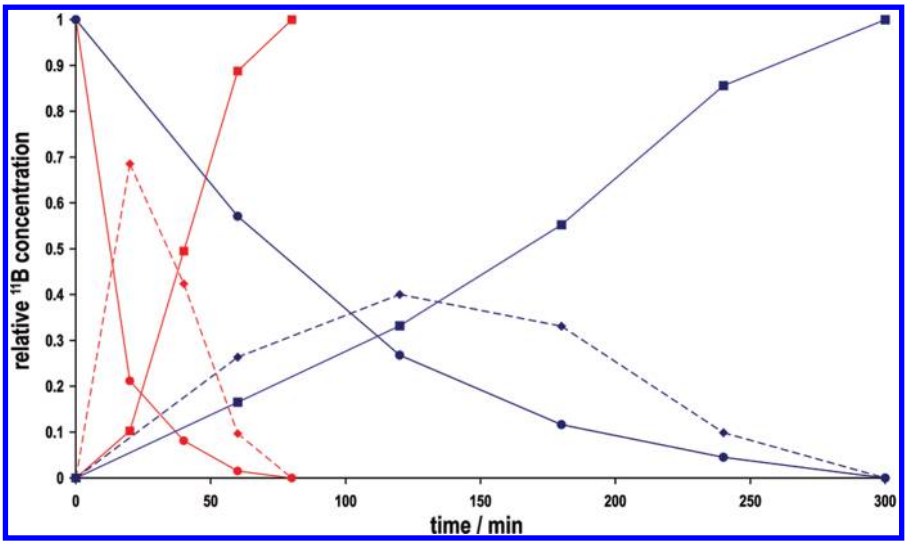

Figure 7. Plot of ^{11}B concentration for the dehydrocoupling of $H_3B{\cdot}NHMe_2$ (initial concentration = 0.072 M) using $[Rh(PR_3)_2(\eta^6\text{-}C_6H_5F)][BAr^F{}_4]$: 5 mol %, 1,2-$F_2C_6H_4$, 298 K. R = ^{i}Pr, blue; R = ^{i}Bu, red. ● = $H_3B{\cdot}NHMe_2$, ■ = $[H_2BNMe_2]_2$, ♦ = $H_3B{\cdot}NMe_2BH_2{\cdot}NHMe_2$.

a slow flow of argon (i.e., not in a sealed tube) by periodic sampling and ^{11}B NMR spectroscopy revealed that, at a loading of 5 mol %, catalysis was complete in 300 min, ToF 4 h^{-1}. This is considerably slower than found for $[Rh(P^iBu_3)_2(\eta^6\text{-}C_6H_5F)][BAr^F{}_4]$ under the same conditions (80 min for 100% completion, ToF 15 h^{-1}),[56] although both are much slower than the current best-reported systems for amine borane dehydrocoupling.[6,14,17] Inspection of a time−^{11}B concentration plot (Figure 7) also demonstrates the growth and disappearance of an intermediate boron-containing species, identified as the linear diborazine $H_3B{\cdot}NMe_2BH_2{\cdot}NHMe_2$.[27,57,58] This has recently been observed by us in the P^iBu_3 catalyst system,[24] shown by Manners and co-workers to be a plausible intermediate in the dehydrocoupling of $H_3B{\cdot}NHMe_2$ as catalyzed by colloidal rhodium,[27] and most recently observed by Schneider and co-workers in the dehydrocoupling of $H_3B{\cdot}NHMe_2$ by bifunctional Ru catalysts.[29] Under the conditions of a sealed NMR tube, after ca. 30% (10 h) *and* 70% (48 h) conversion during catalysis, there is only one organometallic species observed by $^{31}P\{^1H\}$ NMR spectroscopy (~98% detection limit), the chemical shift of which is very close to **3** [δ 67.4, J(RhP) 109 Hz], suggesting its formulation as $[Rh(H)_2(P^iPr_3)_2(\eta^2\text{-}H_3B{\cdot}NHMe_2)][BAr^F{}_4]$ (**5**) and that this is a resting state during the catalytic cycle. Other ^{1}H and ^{11}B NMR data are consistent with this assignment, as is ESI-MS (obsd, 484.2832; calcd, 484.2880 for $[Rh(H)_2(P^iPr_3)_2(\eta^2\text{-}H_3B{\cdot}NHMe_2)]^+$, Figure S-4, Supporting Information). This differs for the P^iBu_3 system in which the analogous complex, **IIa**, is observed but at only ca. 20% composition in an otherwise complex mixture during catalysis.[24]

3. Discussion

In this paper and the previous one,[24] a number of amine− and dimeric amino−borane σ complexes of Rh(I), $\{RhL_2\}^+$, and Rh(III), $\{Rh(H)_2L_2\}^+$, fragments have been prepared where the phosphine ligand (L = P^iBu_3 versus P^iPr_3) and σ ligand ($H_3B{\cdot}NMe_3$, $[H_2BNMe_2]_2$) are varied. This allows for the resulting structures (solution and solid state), reactivity (loss of H_2), and efficacy in the dehydrocoupling of $H_3B{\cdot}NHMe_2$ to be compared. From this, three general observations can be drawn: (*i*) that the σ ligands in the Rh(I) complexes appear to be more tightly bound when L = P^iPr_3 over L = P^iBu_3 and all Rh···B distances are shorter than found in the Rh(III)−dihydride complexes; (*ii*) when L = P^iPr_3, the Rh(III) dihydride amine−borane σ complexes are relatively more stable towards H_2 loss than when L = P^iBu_3; (*iii*) the L = P^iPr_3 ligated complexes are considerably slower in mediating the dehydrocoupling of $H_3B{\cdot}NHMe_2$ than their P^iBu_3 analogs. We discuss these observations in turn.

For the Rh(I) complexes, the larger cone angle of P^iPr_3 (160°) versus P^iBu_3 (143°)[47] is consistent with a larger P−Rh−P angle in **1** and **2** when compared with **Ib** and **III** (Table 1) but is, at first glance, at odds with the tighter Rh−H−B interaction for the P^iPr_3 complexes in both solution and the solid state. This suggests that steric pressure between the phosphine and amine−borane has little to do with modulating this interaction in these particular Rh(I) species. Considering electronic factors, a qualitative Walsh diagram for a linear ML_2 fragment that undergoes bending to a C_{2v} geometry is shown in Scheme 5. As it is established that $H_3B{\cdot}L$ complexes are σ donors only, the B−H σ* orbitals being too high in energy,[46] the relative energies of the metal-based LUMO ($1b_1$) and LUMO+1 ($2a_1$) would be expected to be important in determining the strength of the M−H−B interaction on combination with the filled e set[46] (B−H bonding) of the C_{3v} $H_3B{\cdot}NMe_3$ fragment. As Scheme 5 shows, the $1b_1$ orbital drops in energy with increasing L−M−L angle, and in this qualitative approach, a wider P−Rh−P angle would thus lead to a stronger Rh−H−B interaction. This appears to be the case for **1** and **2** when compared with **Ib** and **III** (Table 1). A wider P−Rh−P angle in the P^iPr_3 complexes that leads to a shorter Rh−B distance would also induce a larger change in chemical shift on coordination of the borane to the metal fragment in both ^{1}H and ^{11}B NMR spectra—as is observed.

The observations regarding the relative stabilities for the Rh(III)−dihydrides **3**, **4**, and **IIb** also are at first inspection counterintuitive: the *bulkier* trans-orientated P^iPr_3 ligands

(56) Under the same loading, but approximately 3 times the concentration (0.2 M), this catalyst gives complete conversion in 35 min, ref 24.
(57) Hahn, G. A.; Schaeffer, R. *J. Am. Chem. Soc.* **1964**, *86*, 1503–1504.
(58) Noth, H.; Thomas, S. *Eur. J. Inorg. Chem.* **1999**, 1373–1379.

Scheme 5. Adapted[59,60] Qualitative Walsh Diagram Showing the Frontier Metal Orbitals for the Bending of a ML_2 d^8 Fragment and the HOMO−1 Orbitals of a C_{3v} $H_3B{\cdot}NMe_3$ Ligand[46a]

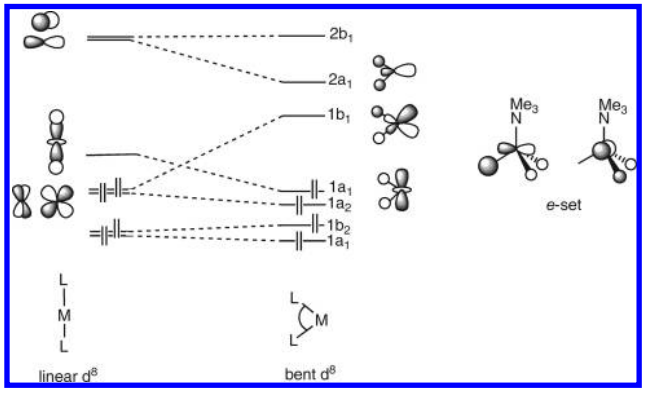

[a]Energies are approximate, and the specific ordering is for illustration only.

lead to a more stable Rh(III)−dihydride, that is, **3** versus **IIb**, and **4** can be isolated (albeit only in the solid state) whereas the P^iBu_3 analog cannot, although relative solubilites might also play a part in the latter. It is well established that L−M−L bite angles exert a significant influence on reductive elimination, and oxidative addition reactions at metal centers[61,62] and P^iBu_3, with its smaller cone angle, allows a tighter P−Rh−P angle in the Rh(III) dihydride that could encourage H_2 reductive elimination. Dubois and co-workers have reported that phosphine bite angles play an important role in determining the position of equilibrium on the addition of H_2 to $[Rh(L_2)_2]^+$ cations (L_2 = chelating diphosphine), with a small bite angle favoring the reductive elimination of H_2, while those with a larger bite angle favor the formation of $[Rh(H)_2(L_2)_2]^+$.[63] Although a direct comparison between the DuBois system and ours is not appropriate given the difference in ligand sets, consideration of the role of the P−Rh−P angle does thus appear to be important when determining relative stabilities of dihydride species bound with these σ ligands. In addition, agostic interactions from the phosphines could lower the energy of the transition state for H_2 elimnation from the Rh(III) intermediates by stabilization of a low-coordinate structure formed during H_2 loss. In support of this, we have previously reported that **VIII**—which in the solid state shows Rh···HC agostic interactions—readily loses H_2 in solution, whereas **IX** does not, although we do not have a solid-state structure for the latter.[64] Caulton and co-workers have previously commented on the role that agostic interactions from phosphine ligands might play in promoting H_2 loss from iridium(III)−dihydride species.[65]

The reasons behind the slower catalysis for $H_3B{\cdot}NHMe_2$ dehydrogenation when compared with P^iBu_3 analogs remain to be fully determined, although stabilization of the P^iPr_3 ligated complexes (as observed for **1** and **3**) that lead to an increased barrier to BH/NH activation or H_2 loss would be expected to slow the rate of catalysis if these steps were either rate-determining or pooled species outside the catalytic cycle. An analysis of relative contributions from these and other factors is complicated significantly by the fact that the dehydrogenation pathway of $H_3B{\cdot}NHMe_2$, to initially give $H_2B{=}NMe_2$, has been calculated to proceed via a number of energetically similar pathways,[24] and the onward reactivity of this unsaturated fragment to ultimately give dimeric $[H_2BNMe_2]_2$ can also proceed via a number of pathways.[29] Nevertheless, the empirical observation that changing the phosphine alters the rate of dehydrocoupling (albeit slower) is an encouraging one for future rational catalyst design.

4. Experimental Section

All manipulations, unless otherwise stated, were performed under an atmosphere of argon, using standard Schlenk and glovebox techniques. Glassware was oven-dried at 130 °C overnight and flamed under a vacuum prior to use. CH_2Cl_2, MeCN, and pentane were dried using a Grubbs-type solvent purification system (MBraun SPS-800) and degassed by successive freeze−pump−thaw cycles.[66] CD_2Cl_2 and 1,2-$C_6H_4F_2$ were distilled under a vacuum from CaH_2 and stored over 3 Å molecular sieves. $H_3B{\cdot}NMe_3$ and $H_3B{\cdot}NMe_2H$ were purchased from Aldrich and sublimed before use. $[Rh(C_6H_5F)(P^iPr_3)_2][BAr^F{}_4]$,[48] $[Rh(C_6H_5F)(P^iBu_3)_2][BAr^F{}_4]$,[64] $[Rh(H)_2(P^iPr_3)_2][BAr^F{}_4]$,[54] $[Rh(NBD)(P^iPr_3)_2][BAr^F{}_4]$,[54] and $[H_2BNMe_2]_2$[27] were prepared according to literature methods. All other chemicals are commercial products and were used as received. NMR spectra were recorded on a Varian Unity or a Bruker AVC 500 MHz spectrometer at room temperature, unless otherwise stated. Chemical shifts are quoted in parts per million and coupling constants in hertz. ESI-MS were recorded on a Bruker MicroOTOF-Q instrument.[67] Microanalyses were performed by Elemental Microanalysis Ltd.

$[Rh(\eta^2\text{-}H_3B{\cdot}NMe_3)(P^iPr_3)_2][BAr^F{}_4]$ (1). To a Schlenk flask charged with $[Rh(C_6H_5F)(P^iPr_3)_2][BAr^F{}_4]$ (0.091 g, 0.066 mmol) and $H_3B{\cdot}NMe_3$ (0.005 g, 0.069 mmol) was added 1,2-$C_6H_4F_2$ (2 mL). The resulting purple solution was stirred at room temperature for 5 min and then layered with pentane and held at 5 °C for 72 h to afford the product as purple crystals. Yield: 0.058 g (65%). Complex **1** is prepared quantitatively in situ by the addition of a slight excess of $H_3B{\cdot}NMe_3$ to $[Rh(C_6H_5F)(P^iPr_3)_2][BAr^F{}_4]$ in 1,2-$C_6H_4F_2$.

^{1}H NMR (CD_2Cl_2, 500 MHz): δ 7.70−7.74 (m, 8H, B$\underline{Ar}^F{}_4$), 7.56 (br, 4H, B$\underline{Ar}^F{}_4$), 2.81 (s, 9H, N$\underline{Me}$), 1.99 (apparent octet,† $J \sim 7$, 6H, P$\underline{CH}$; {^{31}P@δ = 73.9} sept, $^3J_{HH}$ = 7.2), 1.30 (apparent dd,† $J \sim 14$, $J \sim 7$, 36H, PC$\underline{Me}$; {^{31}P@δ = 73.9} d, $^3J_{HH}$ = 7.2), −3.09 (partially collapsed q,‡ fwhm = 290 Hz, $^1J_{BH}$ = 80,‡ 3H, B$\underline{H}$; {^{11}B} δ −3.09, br s, fwhm = 60). [†These signals are observed as complicated second-order multiplets that collapse on ^{31}P decoupling. ‡This resonance appears as a broad doublet with $J \sim 100$. $^1J_{BH}$ from the ^{11}B NMR spectrum.] ^{1}H NMR (CD_2Cl_2, 500 MHz, 200 K): δ 7.71−7.76 (m, 8H, B$\underline{Ar}^F{}_4$), 7.56 (br, 4H, B$\underline{Ar}^F{}_4$), 2.76 (s, 9H, N$\underline{Me}$), 1.89 (apparent octet, $J \sim 7$, 6H, P$\underline{CH}$), 1.23 (apparent dd, $J \sim 13$, $J \sim 7$, 36H, PC$\underline{Me}$), −6.85 (vbr, fwhm = 460 Hz, 2H, Rh$\underline{H}$B). The remaining BH signal was not observed, presumably as it was very broad. ^{1}H NMR (CD_2Cl_2, 500 MHz, 190 K): δ 7.71−7.76 (m, 8H, B$\underline{Ar}^F{}_4$), 7.55 (br, 4H, B$\underline{Ar}^F{}_4$), 4.43 (vbr, fwhm = 350 Hz, 1H, B$\underline{H}$), 2.75 (s, 9H, N$\underline{Me}$), 1.87 (apparent octet, $J \sim 7$, 6H,

(59) Albright, T. A.; Burdett, J. K.; Whangbo, M. H. *Orbital Interactions in Chemistry*; Wiley: New York, 1985.
(60) Su, M. D.; Chu, S. Y. *Inorg. Chem.* **1998**, *37*, 3400–3406.
(61) Brown, J. M.; Guiry, P. J. *Inorg. Chim. Acta* **1994**, *220*, 249–259.
(62) Freixa, Z.; van Leeuwen, P. *Dalton Trans.* **2003**, 1890–1901.
(63) DuBois, D. L.; Blake, D. M.; Miedaner, A.; Curtis, C. J.; DuBois, M. R.; Franz, J. A.; Linehan, J. C. *Organometallics* **2006**, *25*, 4414−4419 and references therin.
(64) Douglas, T. M.; Chaplin, A. B.; Weller, A. S. *Organometallics* **2008**, *27*, 2918–2921.
(65) Cooper, A. C.; Huffman, J. C.; Caulton, K. G. *Organometallics* **1997**, *16*, 1974–1978.
(66) Pangborn, A. B.; Giardello, M. A.; Grubbs, R. H.; Rosen, R. K.; Timmers, F. J. *Organometallics* **1996**, *15*, 1518–1520.
(67) Lubben, A. T.; McIndoe, J. S.; Weller, A. S. *Organometallics* **2008**, *27*, 3303–3306.

PCH), 1.22 (apparent dd, $J \sim 13$, $J \sim 7$, 36H, PCMe), −6.91 (vbr, fwhm = 220 Hz, 2H, RhHB). $^{13}C\{^1H\}$ NMR (CD_2Cl_2, 126 MHz): δ 162.3 (q, J_{BC} = 50, BAr^F_4), 135.4 (s, BAr^F_4), 129.4 (qq, J_{FC} = 32, J_{BC} = 3, BAr^F_4), 125.1 (q, J_{FC} = 272, BAr^F_4), 118.0 (apparent sept, J = 4, BAr^F_4), 53.3 (s, NMe), 27.3−27.9 (second-order m, PCH), 21.0 (s, PCMe). ^{11}B NMR (CD_2Cl_2, 160 MHz): δ 28.8 (br q, $^1J_{BH}$ = 80, 1B, $H_3B\cdot NMe_3$), −6.6 (s, 1B, BAr^F_4). ^{11}B NMR (CD_2Cl_2, 160 MHz, 200 K): δ 28.9 (vbr, fwhm = 400 Hz, 1B, $H_3B\cdot NMe_3$), −6.8 (s, 1B, BAr^F_4). $^{31}P\{^1H\}$ NMR (CD_2Cl_2, 202 MHz): δ 73.9 (d, $^1J_{RhP}$ = 180). $^{31}P\{^1H\}$ NMR (CD_2Cl_2, 202 MHz, 200 K): δ 71.8 (d, $^1J_{RhP}$ = 176). $^{31}P\{^1H\}$ NMR (1,2-$C_6H_4F_2$, 202 MHz): δ 73.8 (d, $^1J_{RhP}$ = 180). ESI-MS (CH_2Cl_2, 60 °C, 4.5 kV) positive ion: m/z 496.2823 $[M]^+$ (calcd, 496.2880). Anal. Calcd for $C_{53}H_{66}B_2F_{24}NP_2Rh$ (1359.55 g mol^{-1}): C, 46.82; H, 4.89; N, 1.03. Found: C, 46.82; H, 5.49; N, 1.25.

[Rh{η^2-(H_2BNMe_2)$_2$}(P^iPr_3)$_2$][BAr^F_4] (2). To a Schlenk flask charged with [Rh(C_6H_5F)(P^iPr_3)$_2$][BAr^F_4] (0.060 g, 0.043 mmol) and [H_2BNMe_2]$_2$ (0.0052 g, 0.046 mmol) was added 1,2-$C_6H_4F_2$ (2 mL). The resulting purple solution was stirred at room temperature for 5 min and then layered with pentane and held at 5 °C for 72 h to afford the product as purple crystals. Yield: 0.051 g (85%). Compound **2** is prepared quantitatively in situ by the addition of a slight excess of [H_2BNMe_2]$_2$ to [Rh(C_6H_5F)-(P^iPr_3)$_2$][BAr^F_4] in 1,2-$C_6H_4F_2$.

^1H NMR (CD_2Cl_2, 500 MHz): δ 7.70−7.74 (m, 8H, BAr^F_4), 7.56 (br, 4H, BAr^F_4), 2.70 (vbr, fwhm ∼ 300 Hz, 2H, BH; {^{11}B} br), 2.63 (s, 12H, NMe), 2.10 (apparent octet,† $J \sim 7$, 6H, PCH; {$^{31}P@\delta$ = 68.2} sept, $^3J_{HH}$ = 7.2), 1.37 (apparent dd,† $J \sim 14$, $J \sim 7$, 36H, PCMe; {$^{31}P@\delta$ = 68.2} d, $^3J_{HH}$ = 7.2), −6.50 (apparent qt,‡ $^1J_{BH}$ = 89.0, $^1J_{RhH}$ = 30.7, $^2J_{PH}$ = 30.4, 2H, RhHB; {^{11}B} apparent t, $J \sim 30$; {$^{31}P@\delta$ = 68.2} qd, $^1J_{BH}$ = 89.0, $^1J_{RhH}$ = 30.7). [†These signals are observed as complicated second-order multiplets that collapse on ^{31}P decoupling. ‡This complex AA′MNXX′ signal was simulated using gNMR[49] to extract the corresponding spectral parameters.] $^{13}C\{^1H\}$ NMR (CD_2Cl_2, 126 MHz): δ 162.3 (q, J_{BC} = 50, BAr^F_4), 135.4 (s, BAr^F_4), 129.4 (qq, J_{FC} = 32, J_{BC} = 3, BAr^F_4), 125.1 (q, J_{FC} = 273, BAr^F_4), 118.0 (apparent sept, J = 4, BAr^F_4), 51.2 (s, NMe), 27.9−28.5 (second-order m, PCH), 21.1 (s, PCMe). ^{11}B NMR (CD_2Cl_2, 160 MHz): δ 35.3 (t, $^1J_{BH}$ = 89, 1B, RhH$_2$B), 5.3 (t, $^1J_{BH}$ = 112, 1B, BH), −6.6 (s, 1B, BAr^F_4). $^{31}P\{^1H\}$ NMR (CD_2Cl_2, 202 MHz): δ 68.2 (d, $^1J_{RhP}$ = 177). $^{31}P\{^1H\}$ NMR (1,2-$C_6H_4F_2$, 202 MHz): δ 68.2 (d, $^1J_{RhP}$ = 178). ESI-MS (CH_2Cl_2, 60 °C, 4.5 kV) positive ion: m/z 537.3316 $[M]^+$ (weak peak, calcd, 537.3316). Anal. Calcd for $C_{54}H_{70}B_3F_{24}N_2P_2Rh$ (1400.41 g mol^{-1}): C, 46.31; H, 5.04; N, 2.00. Found: C, 46.30; H, 4.88; N, 2.06.

***trans*-[Rh(P^iPr_3)$_2$(MeCN)$_2$][BAr^F_4]$_2$.** To a Schlenk flask charged with [Rh(C_6H_5F)(P^iPr_3)$_2$][BAr^F_4] (0.055 g, 0.043 mmol) was added MeCN (0.011 mL, 0.22 mmol) followed by CH_2Cl_2 (2 mL). The resulting yellow solution was stirred at room temperature for 48 h and recrystallized from CH_2Cl_2/pentane. Yield: 0.040 g (68%). Alternatively prepared by the addition of excess MeCN to **1** or **2**.

^1H NMR (CD_2Cl_2, 500 MHz): δ 7.70−7.74 (m, 8H, BAr^F_4), 7.56 (br, 4H, BAr^F_4), 2.11−2.22 (second-order multiplet,† 6H, PCH; {$^{31}P@\delta$ = 42.7} δ 2.17, sept, $^3J_{HH}$ = 7.2), 2.17 (td, $^5J_{PH}$ = 1.7, $^4J_{RhH}$ = 0.7, 6H, MeCN), 1.33 (apparent q,† $J \sim 7$, 36H, PCMe; {$^{31}P@\delta$ = 42.7} d, $^3J_{HH}$ = 7.2). [†These signals are observed as complicated second-order multiplets that collapse on ^{31}P decoupling.] $^{13}C\{^1H\}$ NMR (CD_2Cl_2, 126 MHz): δ 163.9 (q, J_{BC} = 50, BAr^F_4), 136.6 (br, BAr^F_4), 130.6 (qq, J_{FC} = 32, J_{BC} = 3, BAr^F_4), 126.4 (br d, J = 13.4, MeCN), 126.2 (q, J_{FC} = 275, BAr^F_4), 119.0 (apparent sept, J = 4, BAr^F_4), 23.3 (t, $^{1,3}J_{PC}$ = 10, PCH), 19.4 (s, PCMe), 3.9 (s, MeCN). $^{31}P\{^1H\}$ NMR (CD_2Cl_2, 202 MHz): δ 42.6 (d, $^1J_{RhP}$ = 128). ESI-MS (CH_2Cl_2, 60 °C, 4.5 kV) positive ion: m/z 505.2347 $[M]^+$ (calcd, 505.2348). Anal. Calcd for $C_{54}H_{60}BF_{24}N_2P_2Rh$ (1368.71 g mol^{-1}): C, 47.39; H, 4.42; N, 2.05. Found: C, 47.21; H, 3.94; N, 2.38.

[Rh(H)$_2$(η^2-$H_3B\cdot NMe_3$)(P^iPr_3)$_2$][BAr^F_4] (3). To a Schlenk flask charged with [Rh(H)$_2$(P^iPr_3)$_2$][BAr^F_4] {prepared by the hydrogenation (1 atm) of [Rh(NBD)(P^iPr_3)$_2$][BAr^F_4] (0.100 g, 0.073 mmol) in CH_2Cl_2, followed by removal of the solvent in vacuo}[54] and $H_3B\cdot NMe_3$ (0.0056 g, 0.077 mmol) was added 1,2-$C_6H_4F_2$ (2 mL). The resulting yellow solution was stirred at room temperature for 5 min, then layered with pentane and held at 5 °C for 72 h to afford the product as colorless crystals. Yield: 0.065 g (65%). Compound **3** is prepared quantitatively in situ by the hydrogenation (1 atm) of [Rh(η^2-$H_3B\cdot NMe_3$)(P^iPr_3)$_2$]-[BAr^F_4] in 1,2-$C_6H_4F_2$.

^1H NMR (CD_2Cl_2, 500 MHz): δ 7.70−7.74 (m, 8H, BAr^F_4), 7.56 (br, 4H, BAr^F_4), 2.76 (s, 9H, NMe), 2.14−2.26 (second-order m,† 6H, PCH; {$^{31}P@\delta$ = 64.5} sept, $^3J_{HH}$ = 7.1), 1.30 (apparent q,† $J \sim 7$, 36H, PCMe; {$^{31}P@\delta$ = 64.5} d, $^3J_{HH}$ = 7.1), −0.57 (partially collapsed q,‡ fwhm = 260 Hz, $^1J_{BH}$ = 80,‡ 3H, BH; {^{11}B} δ −0.57, d, J = 11, fwhm = 24), −19.75 (dt, $^1J_{RhH}$ = 21.6, $^2J_{PH}$ = 14.6, 2H, RhH; {$^{31}P@\delta$ = 64.5} d, $^2J_{RhH}$ = 21.8). [†These signals are observed as complicated second-order multiplets that collapse on ^{31}P decoupling. ‡This resonance appears as a broad doublet with $J \sim 110$. $^1J_{BH}$ from the ^{11}B NMR spectrum.] ^1H NMR (CD_2Cl_2, 500 MHz, 200 K): δ 7.70−7.75 (m, 8H, BAr^F_4), 7.55 (br, 4H, BAr^F_4), 2.71 (s, 9H, NMe), 2.06−2.18 (second-order m, 6H, PCH), 1.23 (apparent q, $J \sim 7$, 36H, PCMe), −0.79 (vbr, fwhm = 150 Hz, 3H, BH), −19.56 (dt, $^1J_{RhH}$ = 21.5, $^2J_{PH}$ = 14.2, 2H, RhH). No significant change is observed on cooling further to 190 K. $^{13}C\{^1H\}$ NMR (CD_2Cl_2, 126 MHz): δ 162.3 (q, J_{BC} = 50, BAr^F_4), 135.4 (br, BAr^F_4), 129.4 (qq, J_{FC} = 32, J_{BC} = 3, BAr^F_4), 125.1 (q, J_{FC} = 272, BAr^F_4), 118.0 (apparent sept, J = 4, BAr^F_4), 53.9 (obscured, NMe), 26.7 (td, $^{1,3}J_{PC}$ = 12, $^2J_{RhC}$ = 1, PCH), 20.8 (dd, $^2J_{PC}$ = 2, J = 1, PCMe). ^{11}B NMR (CD_2Cl_2, 160 MHz): δ 5.0 (br q, $^1J_{BH}$ = 80, 1B, $H_3B\cdot NMe_3$), −6.6 (s, 1B, BAr^F_4). ^{11}B NMR (CD_2Cl_2, 160 MHz, 200 K): δ 5.4 (vbr, fwhm = 380 Hz, 1B, $H_3B\cdot NMe_3$), −6.7 (s, 1B, BAr^F_4). $^{31}P\{^1H\}$ NMR (CD_2Cl_2, 202 MHz): δ 64.5 (d, $^1J_{RhP}$ = 111). $^{31}P\{^1H\}$ NMR (CD_2Cl_2, 202 MHz, 200 K): δ 63.7 (d, $^1J_{RhP}$ = 111). $^{31}P\{^1H\}$ NMR (1,2-$C_6H_4F_2$, 202 MHz): δ 64.6 (d, $^1J_{RhP}$ = 111). ESI-MS (CH_2Cl_2, 60 °C, 4.5 kV) positive ion: m/z 425.1902 $[M - H_3B\cdot NMe_3]^+$ (calcd, 425.1973). Anal. Calcd for $C_{53}H_{68}B_2F_{24}NP_2Rh$ (1361.57 g mol^{-1}): C, 46.75; H, 5.03; N, 1.03. Found: C, 46.62; H, 5.01; N, 1.12.

[Rh(H)$_2${η^2-(H_2BNMe_2)$_2$}(P^iPr_3)$_2$][BAr^F_4] (4). A solution of [Rh{η^2-(H_2BNMe_2)$_2$}(P^iPr_3)$_2$][BAr^F_4] (0.040 g, 0.029 mmol) in 1,2-$C_6H_4F_2$ (2 mL) was placed under hydrogen (4 atm). The resulting pale yellow solution was left to stand for 5 min and then layered with pentane under hydrogen (1 atm) and held at 5 °C for 72 h to afford the product as colorless crystals. Yield ∼ 0.01 g (25%). NMR spectra of this material dissolved in CD_2Cl_2 at 225 K indicate complete dissociation of [H_2BNMe_2]$_2$; only [Rh(H)$_2$(P^iPr_3)$_2$][BAr^F_4] and free [H_2BNMe_2]$_2$ are seen. Complex **4** is unstable in the absence of hydrogen and converts to **2** over days in the solid state under an argon atmosphere. This process is accelerated by placing the sample under a vacuum. Characterization was carried by X-ray crystallography on this material. Compound **4** can alternatively be prepared by the hydrogenation of **2** in the solid state (4 atm, 48 h).

[Rh(H)$_2$(P^iPr_3)$_2$][BAr^F_4] (IX). Prepared as previously described.[54]

^1H NMR (1,2-$C_6H_4F_2$, 500 MHz): δ 8.33 (br, 8H, BAr^F_4), 7.69 (br, 4H, BAr^F_4), 2.28 (br, 6H, PCH), 1.24 (apparent q, $J \sim 7$, 36H, PCMe), −26.91 (br d, $^1J_{RhH}$ = 40, 2H, RhH). $^{31}P\{^1H\}$ NMR (1,2-$C_6H_4F_2$, 202 MHz): δ 60.2 (d, $^1J_{RhP}$ = 112).

NMR Experiments.

1. Reaction of 1, 2, and 3 with MeCN.

a. To a solution of **1**/**2** (0.008 g, 0.0059/0.0057 mmol) in CD_2Cl_2 (0.4 mL) in a J. Young NMR tube was added MeCN

Table 2. Crystallographic Data

	1	**2**	*trans*-[Rh(P^iPr_3)$_2$(NCMe)$_2$][BAr^F_4]	**3**	**4**
formula	$C_{53}H_{66}B_2F_{24}NP_2Rh$	$C_{54}H_{70}B_3F_{24}N_2P_2Rh$	$C_{54}H_{60}BF_{24}N_2P_2Rh$	$C_{53}H_{68}B_2F_{24}NP_2Rh$	$C_{54}H_{72}B_3F_{24}N_2P_2Rh$
M	1359.54	1400.40	1368.70	1361.55	1402.42
cryst syst	triclinic	triclinic	monoclinic	triclinic	tetragonal
space group	$P\bar{1}$	$P\bar{1}$	$P2_1/c$	$P\bar{1}$	$P4_12_12$
T [K]	150(2)	150(2)	150(2)	150(2)	220(2)
a [Å]	12.4906(2)	12.76990(10)	20.75950(10)	12.4135(2)	13.6939(7)
b [Å]	13.4472(2)	19.72410(10)	29.7418(2)	13.8862(3)	
c [Å]	19.3634(3)	27.1519(2)	21.3100(2)	19.2604(4)	34.408(3)
α [deg]	77.0895(6)	73.7772(2)		105.4259(10)	
β [deg]	86.5573(6)	86.7370(3)	108.5254(5)	104.2746(10)	
γ [deg]	82.4775(5)	73.2126(3)		90.2780(8)	
V [Å^3]	3141.25(8)	6284.63(7)	12475.6(2)	3092.79(10)	6452.3(7)
Z	2	4	8	2	4
density [g cm^{-3}]	1.437	1.480	1.457	1.462	1.444
μ (mm^{-1})	0.428	0.431	0.433	0.435	0.420
θ range [deg]	$5.14 \le \theta \le 26.37°$	$5.11 \le \theta \le 26.37°$	$5.09 \le \theta \le 26.37°$	$5.10 \le \theta \le 26.37°$	$5.11 \le \theta \le 25.03°$
reflns collected	19950 [R_{int} = 0.0182]	44379 [R_{int} = 0.0189]	46573 [R_{int} = 0.0476]	20886 [R_{int} = 0.0244]	6046 [R_{int} = 0.0345]
completeness	97.3%	99.1%	99.1%	98.7%	88.1%
no. of data/restraints/params	12518/715/946	25462/1074/1818	25306/1773/1913	12505/592/978	4435/980/517
R_1 [$I > 2\sigma(I)$]	0.0428	0.0408	0.0518	0.0443	0.0692
wR_2 [all data]	0.1087	0.1037	0.1360	0.1142	0.1702
GoF	1.028	1.021	1.024	1.020	1.057
largest diff. peak and hole [e Å^{-3}]	1.165 and −0.742[a]	0.764 and −0.855	0.624 and −0.569	0.709 and −0.555	0.596 and −0.476

[a] The presence of a relatively large Fourier peak (1.16 e Å^{-3}) near the metal center in this structure is attributed to Fourier truncation errors. If this peak is excluded, the max/min residual density is 0.73/−0.74.

(5 μL, excess), resulting in an immediate change in color from purple to bright yellow. An intermediate species, *cis*-[Rh(P^iPr_3)$_2$(NCMe)$_2$][BAr^F_4] {δ_{31P} 53.4, d, $^1J_{RhP}$ = 179}, was observed initially by ^{1}H and ^{31}P NMR spectroscopy, which subsequently converted to *trans*-[Rh(P^iPr_3)$_2$(NCMe)$_2$][BAr^F_4] (pale yellow solution) quantitatively over ca. 30 min. Free $H_3B{\cdot}NMe_3$ and [H_2BNMe_2]$_2$, respectively, were the only species observed by ^{11}B NMR spectroscopy (with the exception of the anion resonance, [BAr^F_4]$^-$).

b. To a solution of **3** in (0.008 g, 0.0059 mmol) in CD_2Cl_2 (0.4 mL) in a J. Young NMR tube was added MeCN (5 μL, excess) and was immediately analyzed—the formation of [Rh(H)$_2$(P^iPr_3)$_2$(NCMe)$_2$][BAr^F_4], concomitant with the formation of $H_3B{\cdot}NMe_3$, was quantitative by ^{1}H, ^{11}B, and ^{31}P NMR spectroscopy.

2. Reaction of 1 and 2 with H_2.

a. A solution of **1** (0.010 g, 0.0074 mmol) in 1,2-$C_6H_4F_2$ (0.4 mL) was hydrogenated (1 atm) in a J. Young NMR tube and immediately analyzed—the formation of **3** was quantitative by ^{1}H and ^{31}P NMR spectroscopy.

b. A solution of **2** (0.010 g, 0.0071 mmol) in 1,2-$C_6H_4F_2$ (0.4 mL) was hydrogenated (1 atm) in a J. Young NMR tube and then immediately analyzed—the formation of **IX**, concomitant with the formation of [H_2BNMe_2]$_2$, was quantitative as determined by ^{1}H, ^{11}B, and ^{31}P NMR spectroscopy. The hydride signal for **IX** was shifted ca. 8 ppm downfield and broadened (fwhm = 600 Hz) in comparison to isolated material, presumably due to exchange with dissolved H_2.

3. Stability of 3 and 4.

a. A solution of **3** (0.009 g, 0.0066 mmol) in CD_2Cl_2 (0.4 mL) in a J. Young NMR tube was degassed by three successive freeze, pump, and thaw cycles and left to stand for 72 h under a vacuum (5×10^{-3} Torr). No change could be detected by ^{1}H and ^{31}P NMR spectroscopy.

b. A solution of **3** (0.0074 mmol) in 1,2-$C_6H_4F_2$ (0.4 mL) in a J. Young NMR tube, prepared as described above (**1a**), was degassed by three successive freeze, pump, and thaw cycles and placed under argon (no change of color was observed). The addition of $CH_2{=}CH^tBu$ (5 μL, 0.039 mmol) resulted in an immediate change from pale yellow to deep purple, and the quantitative formation of **1** as determined by ^{1}H and ^{31}P NMR spectroscopy ($MeCH_2{}^tBu$ was also observed).

c. A Schlenk flask changed with a crystalline sample of **4** (ca. 0.01 g, prepared as described above by crystallization) under an atmosphere of hydrogen was cooled to 195 K and then placed under argon. The solid was extracted with cold CD_2Cl_2 (195 K) into a J. Young NMR tube, warmed to 225 K, and analyzed by NMR spectroscopy. The quantitative formation of **IX**, contaminant with free [H_2BNMe_2]$_2$, was observed. On warming further to 298 K, a mixture of **IX** and **2** was observed (**1X**/**2** = 1:0.2).

4. Reaction of IX with $H_3B{\cdot}NMe_3$ and [H_2BNMe_2]$_2$. Compound **IX** was prepared by the hydrogenation (1 atm) of [Rh(NBD)(P^iPr_3)$_2$][BAr^F_4] (0.010 g, 0.073 mmol) in CH_2Cl_2 (0.4 mL) in a J. Young NMR tube, followed by the removal of solvent in vacuo.[54]

a. To a solution of **IX** (0.0073 mmol, prepared as described above) in 1,2-$C_6H_4F_2$ (0.4 mL) in a J. Young NMR tube was added $H_3B{\cdot}NMe_3$ (0.001 g, 0.014 mmol) and immediately analyzed—the formation of [Rh(H)$_2$(η^2-$H_3B{\cdot}NMe_3$)(P^iPr_3)$_2$][BAr^F_4] was quantitative by ^{1}H and ^{31}P NMR spectroscopy.

b. To a J. Young NMR tube charged with **IX** (0.0073 mmol, prepared as described above) and [H_2BNMe_2]$_2$ (2, 10, or 50 equiv) was added 1,2-$C_6H_4F_2$ (0.4 mL), resulting in a mixture of **IX** and **2** by ^{1}H and ^{31}P NMR spectroscopy (2 equiv **1X**/**2** = 1:4, 10 equiv **1X**/**2** = 1:10, 50 equiv **1X**/**2** = essentially only 2). A tiny amount of dissolved H_2 (δ 4.7) was observed in each case.

5. Reaction of [Rh(C_6H_5F)(P^iPr_3)$_2$][BAr^F_4] with $H_3B{\cdot}NMe_2H$. To a J. Young NMR tube charged with [Rh(C_6H_5F)(P^iPr_3)$_2$][BAr^F_4] (0.010 g, 0.0072 mmol) and $H_3B{\cdot}NMe_2H$ (0.0043 g, 0.0730 mmol, 10 equiv) was added 1,2-$C_6H_4F_2$ (0.4 mL) to give an initially purple solution, which very rapidly (< 10 s) became colorless. The reaction was then monitored by NMR spectroscopy. After 10 h, conversion of $H_3B{\cdot}NMe_2H$

was ca. 30%; after 48 h, conversion was ca. 70%. $[H_2BNMe_2]_2$ was the major product at both times, and the ***only*** observed metal-containing species at these points was $[Rh(H)_2(\eta^2\text{-}H_3B\cdot NMe_2H)(P^iPr_3)_2][BAr^F{}_4]$—characterized in situ by NMR spectroscopy and ESI-MS. Furthermore, on the basis of ^1H integrals, and within the implied errors associated with their measurement, this rhodium complex is formed in a quantitative amount from the precatalyst (comparison to $[BAr^F{}_4]^-$ integral).

$[Rh(H)_2(\eta^2\text{-}H_3B\cdot NMe_2H)(P^iPr_3)_2][BAr^F{}_4]$ (5). ^1H NMR (1,2-$C_6H_4F_2$, 500 MHz): δ 8.33 (br, 8H, $BAr^F{}_4$), 7.68 (br, 4H, $BAr^F{}_4$), 3.74 (br, 1H, NH), 2.87 (s, 6H, NMe), 2.05−2.15 (second-order m, 6H, PCH), 1.30 (apparent q, $J \sim 7$, 36H, PCMe), −0.97 (vbr, fwhm = 350 Hz, 3H, BH), −18.03 (dt, $^1J_{RhH}$ = 21.0, $^2J_{PH}$ = 13.5, 2H, RhH). ^1H NMR (CD_2Cl_2, 500 MHz, 200 K, selected data): δ −3.56 (br, 2H, RhHB), −18.01 (m, 2H, RhH). ^{11}B NMR (1,2-$C_6H_4F_2$, 160 MHz): δ 3.4 (br, 1B, $H_3B\cdot NMe_2H$), −6.1 (s, 1B, $BAr^F{}_4$). $^{31}P\{^1H\}$ NMR (1,2-$C_6H_4F_2$, 202 MHz): δ 67.4 (d, $^1J_{RhP}$ = 109). $^{31}P\{^1H\}$ NMR (CD_2Cl_2, 202 MHz, 200 K): δ 69.1 (dd, $^2J_{PP}$ = 300, $^1J_{RhP}$ = 109, 1P), 64.9 (dd, $^2J_{PP}$ = 300, $^1J_{RhP}$ = 110, 1P). ESI-MS (1,2-$C_6H_4F_2/CH_2Cl_2$, 60 °C, 4.5 kV) positive ion: m/z 484.2832 $[M]^+$ (calcd, 484.2880).

Dehydrocoupling of $H_3B\cdot NMe_2H$. To a Schlenk flask, connected to an external mineral oil bubbler and charged with a magnetic stirrer bar and the rhodium precursor $[Rh(C_6H_5F)(PR_3)][BAr^F{}_4]$ (R = ^{i}Bu, 0.0265 g, 0.018 mmol; R = ^{i}Pr, 0.0250 g, 0.018 mmol), was added a solution of $H_3B\cdot NMe_2H$ (0.072 M, 5.0 mL, 0.36 mmol, 20 equiv) in 1,2-$C_6H_4F_2$. Reaction progress was monitored by analyzing regular aliquots of the reaction solution (0.1 mL; immediately quenched by the addition of 0.4 mL of MeCN) by ^{11}B NMR spectroscopy. Under these conditions, complete conversion of $H_3B\cdot NMe_2H$ {δ −13.0, q, $^1J_{BH}$ = 96} to $[H_2BNMe_2]_2$ {δ 6.0, t, $^1J_{BH}$ = 112}[27] occurred after 80 min with $[Rh(C_6H_5F)(P^iBu_3)_2][BAr^F{}_4]$ and 300 min with $[Rh(C_6H_5F)(P^iPr_3)_2][BAr^F{}_4]$. The diborazane $[H_3B\cdot NMe_2\text{-}BH_2\cdot NMe_2H]$ {δ 2.9 (t, $^1J_{BH}$ = 109, 1B, BH_2), δ −12.1 (q, $^1J_{BH}$ = 94, 1B, BH_3)}[27] was observed as an intermediate species—no other significant species were observed using ^{11}B NMR spectroscopy under these conditions.

Crystallography. Relevant details about the structure refinements are given in Table 2, and the structures are depicted in Figures 1, 2, 4, 5, and 6. Data were collected on an Enraf Nonius Kappa CCD diffractometer using graphite monochromated Mo Kα radiation (λ = 0.71073 Å) and a low-temperature device.[68] Data were collected using COLLECT; reduction and cell refinement were performed using DENZO/SCALEPACK.[69] The structures were solved by direct methods using SIR2004 (**1**, **2**, *trans*-$[Rh(P^iPr_3)_2(NCMe)_2][BAr^F{}_4]$, **3**)[70] and SHELXS-97 (**4**)[71] and refined full-matrix least-squares on F^2 using SHELXL-97. All non-hydrogen atoms were refined anisotropically. All Rh−H and B−H hydrogen atoms were located on the Fourier difference map (with the exception of H2A and H2B in **4**); their isotropic displacement parameters were fixed to ride on the parent atoms. All other hydrogen atoms were placed in calculated positions using the riding model. The following restraints were applied: B1−H1A = B1−H1B in **1**; B1−H1A = B1−H1B = B11−H11A = B11−H11B in **2**; B1−H1A = B1−H1B in **3**; H0−P1 = H0−P1*; and H1−N1 = H1−N1* in **4** (where * refers to symmetry-related atoms). Disorder of the phosphine ligands in one of the independent molecules in the structure *trans*-$[Rh(P^iPr_3)_2(NCMe)_2][BAr^F{}_4]$ and in one of the phosphine ligands in the structure of **3** was treated by modeling the appropriate substituents over two sites and restraining their geometry. Rotational disorder of the CF_3 groups of the anions was treated by modeling the fluorine atoms over two sites and restraining their geometry. Restraints to thermal parameters were applied where necessary in order to maintain sensible values. Graphical representations of the structures were made with ORTEP3.[72]

Acknowledgment. The EPSRC and the University of Oxford for support.

Supporting Information Available: Figure S-1 to S-4 (selected NMR spectra and ESI-MS). This material is available free of charge via the Internet at http://pubs.acs.org.

(68) Cosier, J.; Glazer, A. M. *J. Appl. Crystallogr.* **1986**, *19*, 105–107.
(69) Otwinowski, Z.; Minor, W. Methods in Enzymology. In *Macromolecular Crystallography, part A*; Carter, C. W., Jr., Sweet, R. M., Eds.; 1997; Vol. *276*, pp 307−326.
(70) Burla, M. C.; Caliandro, R.; Camalli, M.; Carrozzini, B.; Cascarano, G. L.; De Caro, L.; Giacovazzo, C.; Polidori, G.; Spagna, R. *J. Appl. Crystallogr.* **2005**, *38*, 381–388.
(71) Sheldrick, G. M. *Acta Crystallogr., Sect. A* **2008**, *64*, 112–122.
(72) Farrugia, L. *J. Appl. Crystallogr.* **1997**, *30*, 565–565.